

Response of a Warped Flexible Rotor with a Fluid Bearing

Jim Meagher, Professor
Xi Wu, Assistant Professor
Chris Lencioni, Student

Department of Mechanical Engineering
California Polytechnic State University
San Luis Obispo, CA 93407

NOMENCLATURE

A_1, A_2	synchronous response amplitude in planes 1 and 2 (m)
D_1, D_B	damping at inboard disk and outboard journal bearing (N-s/m)
F_1, F_2	forces that bow the shaft (N)
K_1, K_2, K_B	stiffness of shaft segments and journal bearing (N/m)
L_1, L_2	length of shaft segments on either side of disk (m)
M_1, M_2	mass of mid-plane disk and journal mass (kg)
a_o	angular location of bow with respect to imbalance (rad)
e	eccentricity of M_1 (m)
mr_u	imbalance, equivalent to $M_1 e$ (N-m)
Ro	bow factor, ratio of bow to eccentricity ro/e
ro	bow (m)
r_1, r_2	complex displacements in plane 1 and 2
t	time (s)
α_1, α_2	phase (rad)
δ	angular location of mass imbalance at $t=0$.
λ	fluid circumferential average velocity ratio
ω	angular velocity of rotor (rad/s)
j	$\sqrt{-1}$

ABSTRACT

A two complex degrees of freedom model is developed and compared to experimental data for various amounts of rotor bow and its orientation to mass imbalance of the rotor. The equation of motion is developed by adding constant forces that rotate with the rotor to a Bently-Muszynska two-mode isotropic rotor model with a plane journal bearing. Diagnostic information discernable from probes at the bearing is emphasized and compared to midspan response where previous research has concentrated. Good agreement between the analytical model and experiment demonstrate that the analysis presented can be useful to diagnose and balance residual shaft bow from probes located at the bearings where vibration data is typically more available.

1. INTRODUCTION

Rotor bow can be present in large horizontal rotors at rest for long periods, in misaligned rotors, or in rotors where rub causes a thermal bow on the shaft. This can lead to instabilities, difficulty in balancing, and preload on bearings. Nicholas [1], modeled shaft bow with a rotating force similar to imbalance using a Jeffcott rotor model. Peak response and phase angle of bowed rotors were compared to straight shafts for various amounts of bow

and bow orientation. The principal indicators of bow identified were phase angles other than 90 degrees at resonance and phase change variations during acceleration through resonance. Rao [2], using an equivalent analytical model to develop an extensive list of observations that help diagnose the presence of rotor bow. Both of these analytical studies used rigid bearings and the response at midspan which is normally inaccessible. Flack [3] used a transfer matrix method to study bowed rotor response for shafts with five different sets of fluid film bearings. The transfer matrix approach allowed multi-mass rotors to be analyzed. Direct comparisons to experimental data were also conducted for four different types of fluid bearings typically used in industrial turbo machines. Good agreement was reported between experiment and theory but results were limited to midspan motion which is usually not available and only presented the case of imbalance and bow 180° apart. Model-based identification methods have increasingly been used to identify rotor bow [5] but they are necessarily more complicated, machine specific, and less general than the lumped parameter approach used herein.

The objective of this paper is to two-fold: provide a closed form solution for a bowed shaft response that includes a fluid bearing, and to compare mid-plane response to response at the bearing. Numerical methods such as transfer matrices or finite elements allow individual machines to be modeled but they don't easily provide parametric models or predicted responses that are transferable to other machines. Diagnostic information of machinery condition must also be related to transducer measurement and location.

2. ANALYTICAL APPROACH

A Bently-Muszynska model [4] for a two mass system with a fluid bearing was modified to include rotor bow. The rotor model as depicted below has two lumped masses, a mid-span disk and outboard journal, separated by a uniform flexible shaft. The rotor is supported by a stiff bearing inboard and a fluid bearing at the outboard end. The journal mass, M_2 , operates in a fluid bearing characterized with lumped damping, D_B , and bearing stiffness, K_B . The average fluid circumferential velocity, λ , is the ratio of average fluid circumferential angular velocity over shaft angular velocity. An imbalance is modeled at the mid-plane mass and is at an angle a_0 relative to the bow plane. The rotating forces fixed on the shaft that create the bow effect are determined from equilibrium corresponding to residual rotor deflection r_0 at mid-plane.

$$F_1 = (K_1 + K_2)r_0 \quad (1)$$

$$F_2 = \left(\frac{L_1}{L_1 + L_2}\right)F_1 \quad (2)$$

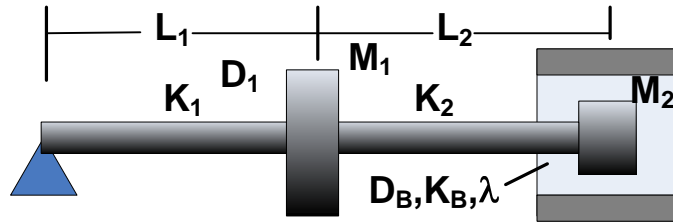


Figure 1 Two mass flexible rotor model

The corresponding equations of motion follow from the dynamic equilibrium depicted in figures 1 and 2:

$$M_1 \ddot{\mathbf{r}}_1 + D_1 \dot{\mathbf{r}}_1 + (K_1 + K_2)\mathbf{r}_1 - K_2 \mathbf{r}_2 = m r_u \omega^2 e^{j(\omega t + \delta)} + F_1 e^{j(\omega t + \delta - a_0)} \quad (3)$$

$$M_2 \ddot{\mathbf{r}}_2 + D_B \dot{\mathbf{r}}_2 + (K_2 + K_B - j D_B \lambda \omega)\mathbf{r}_2 - K_2 \mathbf{r}_1 = F_2 e^{j(\omega t + \delta - a_0 + \pi)} \quad (4)$$

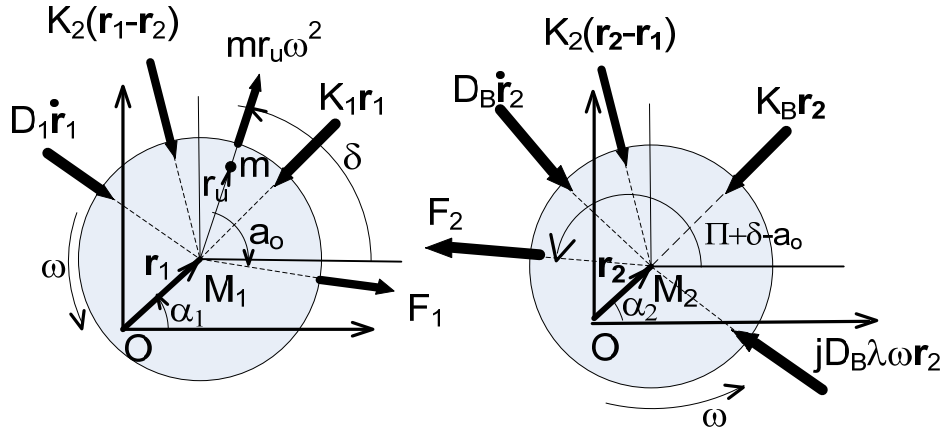


Figure 2 Lumped parameter modeling of forces in each plane.

Assuming solutions of the form:

$$\mathbf{r}_1 = A_1 e^{j(\omega t + \alpha_1)} \quad (5)$$

$$\mathbf{r}_2 = A_2 e^{j(\omega t + \alpha_2)} \quad (6)$$

allows determination of the resulting motion at each mass:

$$A_1 e^{j\alpha_1} = \frac{[K_2 + K_B - M_2 \omega^2 + jD_B(1-\lambda)][mr_u \omega^2 + F_1 e^{-j a_0}] e^{j\delta} + K_2 F_2 e^{j(\delta - a_0 + \pi)}}{[K_1 + K_2 - M_1 \omega^2 + j\omega D_1][K_2 + K_B - M_2 \omega^2 + jD_B \omega(1-\lambda)] - K_2^2} \quad (7)$$

$$A_2 e^{j\alpha_2} = \frac{K_2 [mr_u \omega^2 + F_1 e^{-j a_0}] e^{j\delta} + (K_1 + K_2 - M_1 \omega^2 + j\omega D_1) F_2 e^{j(\delta - a_0 + \pi)}}{[K_1 + K_2 - M_1 \omega^2 + j\omega D_1][K_2 + K_B - M_2 \omega^2 + jD_B \omega(1-\lambda)] - K_2^2} \quad (8)$$

and corresponding phase:

$$\alpha_i = \arctan \left[\frac{\text{Im}(A_i e^{j\alpha_i})}{\text{Re}(A_i e^{j\alpha_i})} \right] \quad i = 1, 2 \quad (9)$$

These equations were solved using Matlab™ for varying amount of bow and various orientations of the bow plane relative to mass unbalance. Single plane theoretical responses for a flexible rotor on stiff bearings are well known [1,2] but the cases presented here were tested experimentally and present results at the bearing where vibration data is more readily available.

3. EXPERIMENTAL APPARATUS

An RK4 Bently Nevada Rotor kit was used for experimental measurements. The rotor is driven through a flexible coupling by an electric motor with a speed controller. The speed range of testing was from a slow roll of 250 rpm up to approximately 3500 rpm where whirl instability was observed. Shaft lateral vibrations were measured with two sets of proximity probes in horizontal and vertical orientations at the mid-span disk and at the fluid journal

bearing. Before testing, a 10 mm rotor was permanently bowed in a hydraulic test machine. The rotor was then carefully balanced in order for the high speed imbalance response to equal the low speed bow response with self balancing at the critical speed. Theoretically for a Jeffcott rotor model this occurs when the bow plane and imbalance are 180° apart with $R_0=1$. As shown in figure 3, this response is accurately modeled by the proposed lumped parameter model except R_0 was set to 0.87 due to differences in predicted response with the current model. This case is used as a baseline for parameter identification. Subsequent simulations for different bow factor and bow orientation use the same parameters except for imbalance orientation and eccentricity which were experimentally modified using additional imbalance masses added to the rotor disk.

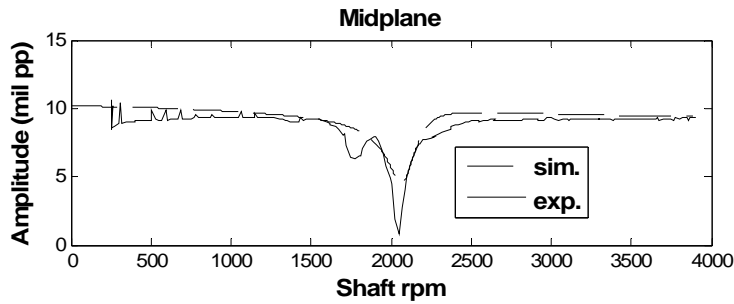


Figure 3 Bowed rotor experimental (exp.) and simulated (sim.) response.

imbalance response and asymptotically approaches the eccentricity. This is as predicted by earlier models [1,2]. The limitation of earlier models is shown in figure 5 where the response at the bearing is depicted. The self balancing speed is no longer evident and the response is not easily identified as a bowed rotor. The low speed response asymptote does not as clearly indicate bow as does the midplane response.

4. RESULTS

The case of self balancing prior to the critical speed is shown in figures 4 and 5. Additional imbalance mass was added opposite the bow plane to increase the eccentricity. At low speeds the bow response is dominant and is characterized by high whirl amplitude. The amplitude reaches a minimum when the bow response and imbalance cancel. After resonance the response is dominated by the

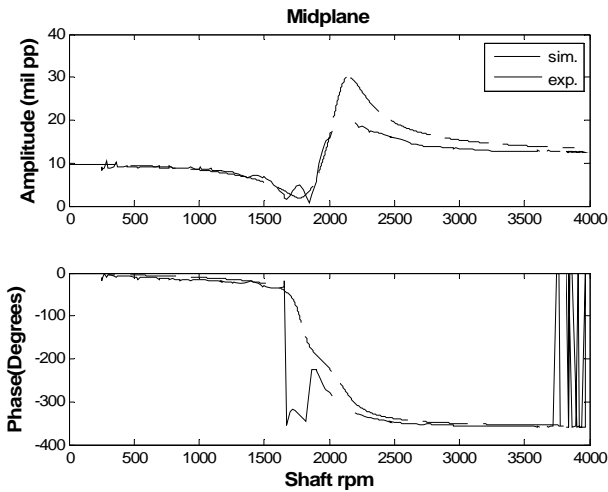


Figure 4 Synchronous response of a bowed rotor at mid-plane disk. $R_0=0.64$, $a_0 = 180^\circ$. Drop out of data near 2000 rpm is due to displacement exceeding transducer range. Phase wrap evident in the experimental plot around 1700 rpm and above 3500 rpm is due to software that adds 360° for phase ranges beyond 360°

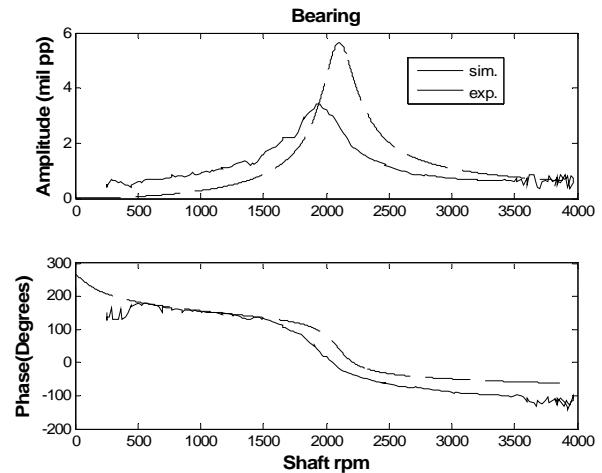


Figure 5 Synchronous response of a bowed rotor at outboard bearing. $R_0=0.64$, $a_0 = 180^\circ$.

Similar differences between mid-plane and outboard measurements occur when masses opposite the bow plane are removed. This increases the bow factor and moves the self balancing speed above the critical speed as

shown in figure 6. Removing imbalance masses increases the bow factor by decreasing the eccentricity. Once again the simulation and experimental response are well matched in both planes but single plane models would not predict the presence of bow from the bearing data.

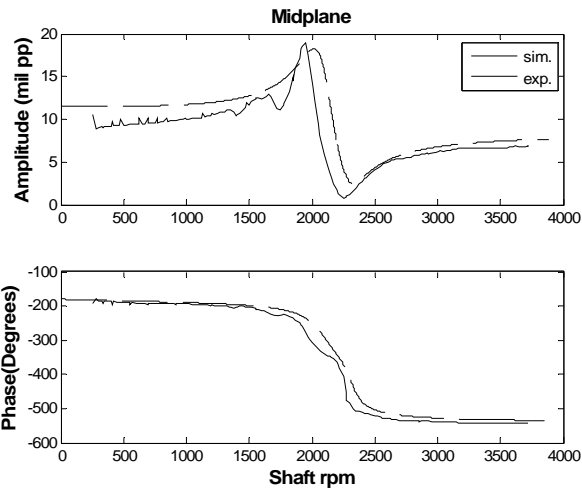


Figure 6 Synchronous response of a bowed rotor at midplane disk. $R_0=1.09$, $a_0 = 180^\circ$.

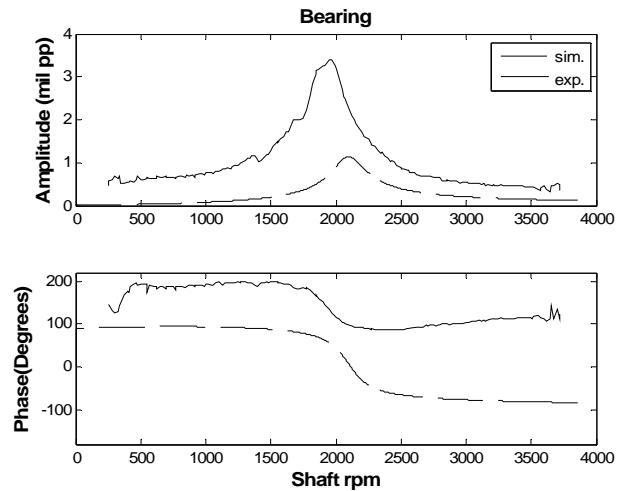


Figure 7 Synchronous response of a bowed rotor at outboard bearing. $R_0=1.09$, $a_0 = 180$ degrees.

Comparing the response at the bearing in figure 7 to that at midplane in figure 6 illustrates the difficulty of diagnosing a bowed rotor from the bearing response.

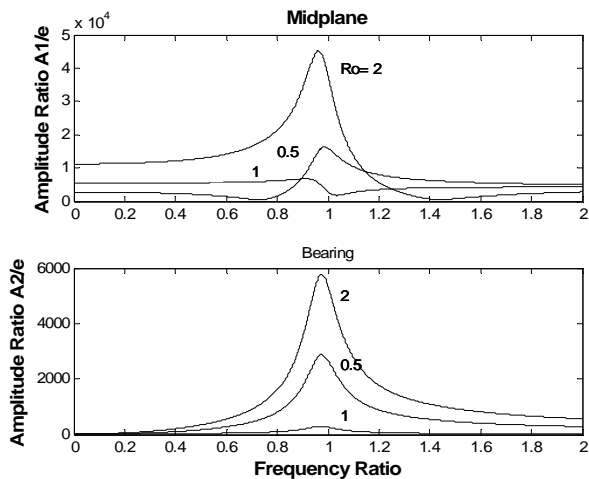
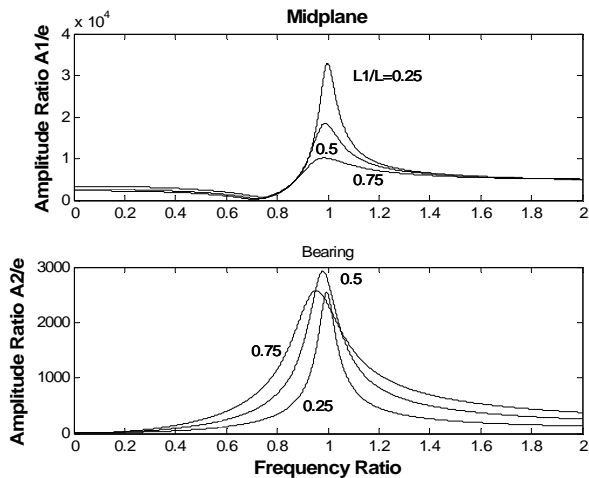


Figure 8 Response curves with bow opposite imbalance for various bow factors, R_0

response indicates increased damping as the central disk approaches the bearing but negligible changes in the peak amplitude.

Theoretical comparison of the vibration amplitude at the midplane to the response at the bearing is shown in figure 8. For each case the minimum response is for bow and eccentricity to be equal with the minimum occurring at the self balancing speed of the midplane. Response at the bearing appears to be solely from eccentricity. For a Jeffcott rotor model the self balancing speed occurs at $\omega^2 = R_0$ for $a_0 = 180^\circ$. This occurs at approximately the same speed when a fluid bearing is present.

Figure 9 illustrates how the position of the central disk along the shaft does not effect the self balancing speed but the midplane peak response decreases with nearness to the outboard bearing. Since an isotropic shaft was assumed $L1/L$ is equivalent to $K_2/(K_1+K_2)$ so that the same effect could be accomplished with changing the shaft segment stiffness. The bearing



**Figure 9 Response curves for various locations of disk.
Ro=0.5, a0=180°**

As shown in figure 10, when the bow plane and imbalance are not 180° apart the response amplitude does not have a self balancing speed. At 0° difference the bow and imbalance act together and have the largest response. The difference between phase measured from midplane probes and outboard probes for different bow plane orientations is illustrated in figures 11. The low speed phase measured at midplane is a good diagnostic for bow location with the phase equal to bow orientation. Self balancing is evident at the midplane disk for a0=180° from the phase jump at frequency ratio 0.7. Phase jump occurs in the special case where bow plane and imbalance are opposite. At zero speed the phase at the bearing lags the bow plane by 90° but as the shaft speed increases the phase changes due to the fluid tangential force, $jD_B \lambda \omega r_2$. The low speed phase change at the bearing varies with bow factor.

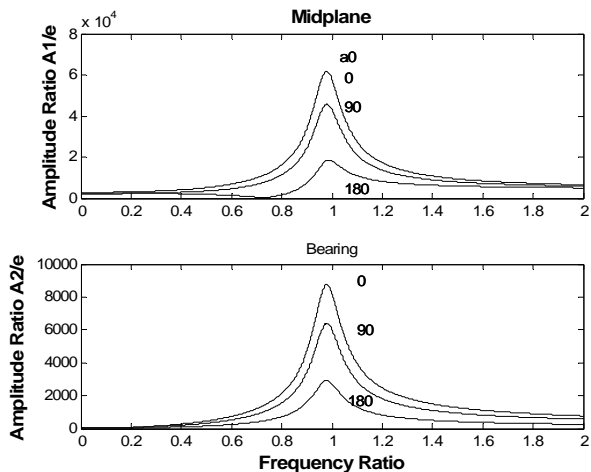


Figure 10 Response amplitude for various bow orientations relative to the imbalance plane. Ro = 0.5.

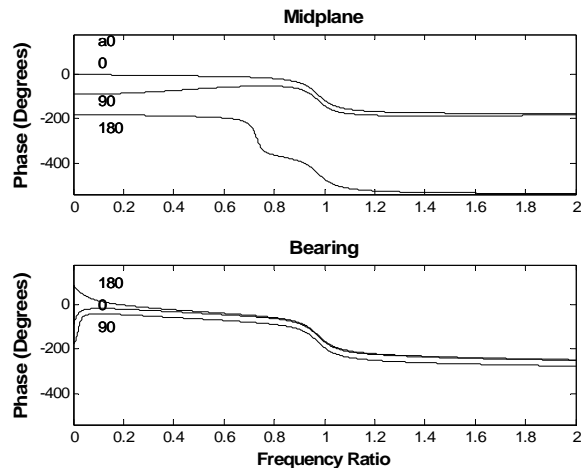


Figure 11 Phase response for various orientations of bow with respect to imbalance. Ro=0.5

5. SUMMARY

A parametric model of a flexible bowed shaft with imbalance is presented. The mathematical model agrees with experimental measurements and extends earlier models by including an outboard fluid bearing with response predicted at the bearing where response data is more typically available. Self balancing predicted by Jeffcott rotors models occurs as well for a rotor with a fluid bearing but is not apparent using probes at the bearing. Diagnostic indicators for bow such as self-balancing or phase jump which can be seen at midspan are not apparent at the bearing. Low speed runout at the bearing can be used to indicate residual rotor bow but it is not as obvious as measurements made from midspan probes. The low speed phase at either the bearing or midspan indicates the bow angle with respect to the imbalance but the phase quickly changes at the bearing due to fluid forces.

ACKNOWLEDGMENTS

The authors wish to acknowledge the support of the Donald E. Bently Center for Engineering Innovation at California Polytechnic State University San Luis Obispo for support of this work.

REFERENCES

1. Nicholas J. C., Gunter E. J., and Allaire P. E., "Effect of Residual Shaft Bow on Unbalance Response and Balancing of a Single Mass Flexible Rotor," *Journal of Engineering for Power* 98, TRANS. ASME., April 1976: 171-181.
2. Rao J.S., "A note on Jeffcott warped rotor," *Mechanism and Machine Theory*, n5, v36, May 2001: 563-575.
3. Flack R.D., and Rooke J.H., "Theoretical-Experimental Comparison of the Synchronous Response of a Bowed Rotor in Five Sets of Fluid Film Bearings," *J. Sound and Vibration* (1980) 73(4), 505-517.
4. Bently D.E., and Hatch C.T., "Fundamentals of Rotating Machinery Diagnostics," *Bently Pressurized Bearing Press* (2002), 200-207.
5. Bachschmid N., Pennacchi P., Vania A., "Identification of Multiple Faults in Rotor Systems," *Journal of Sound and Vibration* (2002) 254(2), 327-366